AFRL-RX-WP-TP-2010-4141

MICROSTRUCTURAL RESPONSE OF PURE COPPER TO CRYOGENIC ROLLING (PREPRINT)

T. Konkova and A. Korznikov

Russian Academy of Science

S. Mironov

Tohoku University

S.L. Semiatin

Metals Branch
Metals, Ceramics & NDE Division

APRIL 2010

AIR FORCE RESEARCH LABORATORY
MATERIALS AND MANUFACTURING DIRECTORATE
WRIGHT-PATTERSON AIR FORCE BASE, OH 45433-7750
AIR FORCE MATERIEL COMMAND
UNITED STATES AIR FORCE

REPORT DOCUMENTATION PAGE

Form Approved
OMB No. 0704-0188

1. REPORT DATE *(DD-MM-YY)*	2. REPORT TYPE	3. DATES COVERED *(From - To)*
April 2010	Conference Paper Preprint	01 April 2010 – 01 April 2010

4. TITLE AND SUBTITLE
MICROSTRUCTURAL RESPONSE OF PURE COPPER TO CRYOGENIC ROLLING (PREPRINT)

5a. CONTRACT NUMBER
In-house

5b. GRANT NUMBER

5c. PROGRAM ELEMENT NUMBER
62102F

6. AUTHOR(S)
T. Konkova and A. Korznikov (Russian Academy of Science)
S. Mironov (Tohoku University)
S.L. Semiatin (AFRL/RXLMP)

5d. PROJECT NUMBER
4347

5e. TASK NUMBER
RG

5f. WORK UNIT NUMBER
M02R2000

7. PERFORMING ORGANIZATION NAME(S) AND ADDRESS(ES)

Russian Academy of Science
Institute for Metals Superplasticity Problems
39 Khalturin Str.
Ufa 450001, Russia

Tohoku University
Department of Materials Processing
Graduate School of Engineering
6-6-02 Aramaki-aza-Aoba
Sendai 980-8579, Japan

Metals Branch (AFRL/RXLM)
Metals, Ceramics & NDE Division
Materials and Manufacturing Directorate
Wright-Patterson Air Force Base, OH 45433-7750
Air Force Materiel Command
United States Air Force

8. PERFORMING ORGANIZATION REPORT NUMBER
AFRL-RX-WP-TP-2010-4141

9. SPONSORING/MONITORING AGENCY NAME(S) AND ADDRESS(ES)
Air Force Research Laboratory
Materials and Manufacturing Directorate
Wright-Patterson Air Force Base, OH 45433-7750
Air Force Materiel Command
United States Air Force

10. SPONSORING/MONITORING AGENCY ACRONYM(S)
AFRL/RXLMP

11. SPONSORING/MONITORING AGENCY REPORT NUMBER(S)
AFRL-RX-WP-TP-2010-4141

12. DISTRIBUTION/AVAILABILITY STATEMENT
Approved for public release; distribution unlimited.

13. SUPPLEMENTARY NOTES
Journal article submitted to *Acta Materialia*. PAO Case Number: 88ABW-2010-1121; Clearance Date: 11 Mar 2010. The U.S. Government is joint author of this work and has the right to use, modify, reproduce, release, perform, display, or disclose the work. Paper contains color.

14. ABSTRACT
A high-resolution electron-back-scatter-diffraction (EBSD) technique was applied to quantify grain-structure development and texture evolution during/after cryogenic rolling of pure copper. Microstructure evolution was found to be a complex process involving mainly geometrical effects associated with strain and discontinuous recrystallization but also including limited twinning and grain subdivision. Recrystallization was deduced to be static in nature and probably occurred during static storage of the material at room temperature after cryogenic rolling. The texture contained a pronounced {110}<112> brass component; this observation was interpreted in terms of the suppression of cross slip at cryogenic temperatures. In general, cryogenic rolling was found to be ineffective for the formation of a nanocrystalline (NC) structure in pure copper.

15. SUBJECT TERMS
cryogenic deformation, nanocrystalline, copper, electron backscatter diffraction, microstructure, texture

16. SECURITY CLASSIFICATION OF:			17. LIMITATION OF ABSTRACT:	18. NUMBER OF PAGES	19a. NAME OF RESPONSIBLE PERSON (Monitor)
a. REPORT	b. ABSTRACT	c. THIS PAGE			Sheldon L. Semiatin
Unclassified	Unclassified	Unclassified	SAR	32	19b. TELEPHONE NUMBER *(Include Area Code)* N/A

Standard Form 298 (Rev. 8-98)
Prescribed by ANSI Std. Z39-18

Microstructural response of pure copper to cryogenic rolling

T. Konkova[1], S. Mironov[1,2], A. Korznikov[1], and S.L. Semiatin[3]

[1]Institute for Metals Superplasticity Problems, Russian Academy of Science, 39 Khalturin Str., Ufa, 450001, Russia
[2]Department of Materials Processing, Graduate School of Engineering, Tohoku University, 6-6-02 Aramaki-aza-Aoba, Sendai 980-8579, Japan
[3]Air Force Research Laboratory, Materials and Manufacturing Directorate, AFRL/RXLM, Wright-Patterson AFB, OH 45433-7817, USA

A high-resolution electron-back-scatter-diffraction (EBSD) technique was applied to quantify grain-structure development and texture evolution during/after cryogenic rolling of pure copper. Microstructure evolution was found to be a complex process involving mainly geometrical effects associated with strain and discontinuous recrystallization but also including limited twinning and grain subdivision. Recrystallization was deduced to be static in nature and probably occurred during static storage of the material at room temperature after cryogenic rolling. The texture contained a pronounced {110}<112> brass component; this observation was interpreted in terms of the suppression of cross slip at cryogenic temperatures. In general, cryogenic rolling was found to be ineffective for the formation of a nanocrystalline (NC) structure in pure copper.

Keywords: Cryogenic deformation; Nanocrystalline; Copper; Electron backscatter diffraction; Microstructure; Texture

1. Introduction

There is currently great interest in the development of structural materials with submicron or nanocrystalline (NC) grain structures. This interest is driven primarily by marked increases in room-temperature strength and improvements in high-temperature ductility. Severe-plastic-deformation (SPD) processes [1] have been found to be among the most effective methods for fabricating such materials. An important limitation of such techniques, however, is the development of an equilibrium (minimum) grain size at high levels of strain [2-3]. Typically, this minimum grain size is of the order of several hundred nanometers and thus lies outside the commonly-defined NC-range of 1-100 nm [2-3]. The reason for the observed grain-refinement stagnation is not completely clear. One possible explanation focuses on the operation of dynamic recovery even at relatively low homologous temperatures. Because recovery is a thermally-activated process, the most-evident method to suppress it (and thus enable further decreases in grain size) comprises deformation at lower temperatures as in the cryogenic range. This approach, known as “cryogenic deformation”, has recently been proposed as a means of producing bulk NC materials [4-10].

To date, the majority of research on SPD processing has focused on aluminum and copper alloys, most likely because of the exceptional ductility of such materials. An analysis of the literature suggests that these materials behave in a distinctly different way under cryogenic-deformation conditions. For example, according to Huang, et al. [4], one of the key mechanisms governing grain-structure evolution in pure aluminum at cryogenic temperatures is the geometrical effect of strain per se. In other words, grains

change their shape in proportion to the imposed strain, and no noticeable gross grain fragmentation/subdivision is observed. By this means, a reasonably homogeneous grain structure, dominated by heavily elongated grains aligned with a direction of the macroscopic material flow, is developed. Such grain structures typically contain a significant proportion of low-angle boundaries (~30%) which have a transverse orientation with respect to the direction of material flow. Of particular importance are the observations that the geometrical grain compression also tends to saturate with strain and the minimum achievable grain size lies in the *submicrocrystalline* range. It has been hypothesized that this effect may be associated with a surprisingly high rate of the thermally-activated grain boundary migration. Thus, the potential of cryogenic deformation for the formation of an NC grain structure in pure aluminum is not clear.

In contrast to the behavior observed for aluminum, a different mode of the microstructure evolution during cryogenic processing has been reported for copper [7-10]. At relatively small strains, extensive twinning takes place [7, 8, 11]. The twins are typically very narrow (~50 nm) and are frequently arranged as twin colonies which efficiently refine the original grains [7, 8]. It is believed that the activation of twinning is mainly associated with the suppression of dislocation cross-slip [8]. As the strain increases, twinning tends to saturate, and shear banding begins to play a major role in grain refinement [7, 8, 11]. The shear bands intersect the twin colonies, thus leading to significant distortion of the original twins [7, 8, 11]. The boundaries outlining the shear bands are found to be essentially straight, and their planes may be close to {111} slip planes [11]. Additionally, the development of adiabatic shear bands may also take place at high strain rates [7, 12]. The peak temperature in these bands may reach ~500K, thus promoting local recrystallization [7, 12].

The activation of mechanical twinning/ shear banding and the grain refinement associated with such deformation mechanisms suggest that cryogenic deformation may be effective for the development of an NC structure in copper. Indeed, the formation of microstructures with an average grain size of ~100 nm has been reported recently in the literature [7, 8]. Because of the exceptionally fine-scale of the grain sizes in such microstructures, much of the information available in the literature to date has been based on transmission electron microscopy (TEM). Despite the excellent resolution of TEM, however, it is unclear whether such results are statistically representative or isolated observations. On the other hand, microstructure observations based on high-resolution electron back-scatter diffraction (EBSD) enable quantification of microstructural features over a much larger scale than TEM and thus provide insights that may be more significant from a statistical viewpoint. The objective of the present work, therefore, was to establish the mechanism(s) of microstructure evolution *during* cryogenic processing of copper and the stability of such microstructures *following* deformation using EBSD. To this end, copper samples were cryogenically rolled to various reductions and examined via EBSD.

2. Material and Experimental Procedures

The program material consisted of copper of 99.9 wt. pct. purity which was received in the form of hot-rolled bar. To increase the probability of obtaining an ultrafine microstructure via cryogenic processing, the as-received bar was pre-conditioned by subjecting cylindrical billets (40 mm diameter $\times$ 70 mm length) to successive height reductions of ~40% along each of the three orthogonal axes (i.e., so-called “abc”-

deformation) in the temperature range of 500-300°C [13]. Samples obtained from this preliminary processing are denoted throughout as the initial material.

Cryogenic rolling was conducted on specimens measuring $45 \times 45 \times 5$ mm^3 that were cut perpendicular to the final compression axis from the central, most severely deformed part of the SPD'ed billets. The specimens were rolled to 50, 75, or 93% overall thickness reductions (true strains of 0.7, 1.4 and 2.7) using a rolling speed of 100 mm/s in a cluster mill with 65-mm diameter work rolls. The total thickness reductions were achieved using multiple passes of ~10% each. In order to provide cryogenic deformation conditions, the rolling specimen and the rolls were soaked in liquid nitrogen prior to each rolling pass and held for 20 minutes; immediately after each pass, the workpiece was re-inserted into liquid nitrogen. The total time for each rolling pass (i.e., the exposure time of a specimen under ambient conditions) was only a few seconds[1]. After completion of the rolling process, specimens were stored at room temperature.

To examine the grain refinement in three dimensions, the rolled specimens were cut for EBSD observations in the plane containing the RD and ND (i.e., the longitudinal plane) as well as the plane containing the RD and TD (i.e., the rolling plane). (In this work, the typical flat-rolling convention is adopted with RD being the rolling direction, TD the transverse direction, and ND the normal direction of the sheet.) Samples were prepared for EBSD by mechanical polishing followed by electro-polishing in a solution of 70% orthophosphoric acid in water at ambient temperature with an applied potential of 5 V. All microstructural and textural observations were made at the mid-thickness of the rolled specimens.

High-resolution EBSD analysis was conducted using a Hitachi S-4300SE field-emission-gun scanning-electron microscope equipped with TSL OIM™ EBSD software. Orientation mapping involving beam control was performed using a triangular scanning grid with step sizes of 0.05-0.5 μm. On each pattern, seven Kikuchi bands were used for indexing, thus minimizing errors. EBSD maps of ~200,000-500,000 points containing ~500-15,000 grains were obtained. Pattern solution efficiency was in the range of 99-100%. The average confidence index (CI) for each EBSD map ranged from 0.15 to 0.66. By comparison, experiments on various FCC materials have shown that the fraction of correctly indexed patterns with CI's greater than 0.1 is 95% [14]. To improve the reliability of the EBSD data, small grains comprising 3 or fewer pixels were automatically removed from the maps using the grain-dilation option in the TSL software. In addition, to eliminate spurious boundaries caused by orientation noise, a lower-limit boundary-misorientation cut-off of 2° was used. All quoted misorientation angles are relative to the rotation axis with the minimum misorientation. A 15° criterion was used to differentiate low-angle boundaries (LABs) and high-angle boundaries (HABs). All measurements of grain size were made by the linear-intercept method.

Transmission electron microscopy (TEM) was performed to further delineate the microstructures developed during and following cryogenic rolling of copper. For this purpose, thin foils were fabricated from rolling-plane sections. Specifically, 3-mm diameter disks were ground to a thickness of ~0.1 mm and then jet-polished in a solution

[1] Heat transfer calculations revealed that the *warming* of the rolls and specimen prior to rolling due to free convection in air was relatively small, resulting in temperature increases of approximately 1-4°C.

containing 7% orthophosphoric acid in water at ~20^{o}C and a voltage of 4 V. TEM was performed using a JEM-2000EX operating at 160 kV.

To establish the effect of cryogenic deformation on mechanical behavior, uniaxial tension tests and microhardness measurements were performed at ambient temperature. Dog-bone tension specimens having a reduced section 12-mm long and 3-mm wide were machined parallel to the RD of ground-and-polished rolled sheet. Room-temperature tension tests to failure were conducted at a constant crosshead speed corresponding to a nominal strain rate of 10^{-3} s^{-1} in an Instron 1185 Universal Testing Machine. Vickers microhardness data were obtained by applying a load of 50g for 10s; at least 10 measurements were made to obtain an average value.

To estimate the stress-strain response of the material during the cryogenic rolling, compression tests were also performed at the liquid nitrogen temperature. To this end, prismatic specimens measuring 6 x 5 x 5 mm^3 were cut from the initial material and compressed in a Schenk universal testing machine at a crosshead velocity of 1 mm/min. During the tests, the dies and specimens were completely immersed in liquid nitrogen.

3. Results and Discussion

3.1. Material prior to cryogenic rolling

Typical microstructural features of the material after warm "abc" deformation (i.e., the initial condition) are summarized in Fig. 1. In the EBSD inverse-pole figure (IPF) map for the normal direction (i.e., the final compression direction), shown in Fig. 1a[2], LABs are depicted as bright lines and HABs as black lines. The IPF map indicated that the initial microstructure was reasonably homogeneous and was dominated by low-aspect-ratio, nearly equiaxed grains. The mean HAB intercepts in the ND and RD were 1.6 and 1.8 μm, respectively. Most of the grain boundaries were high-angle in character (HAB fraction was 59%) but some grains contained dense substructure. The misorientation distribution (Fig. 1b) was characterized by a noticeable low-angle maximum, a weak peak in the vicinity of 60°, and some clustering of misorientation axes near <111>. The fraction of Σ3 twin boundaries was ~5%. The material had a weak nearly-cube texture (Fig. 1c).

3.2. Broad aspects of microstructure evolution

A broad range of microstructural features were noted in the cryogenically-rolled copper samples. These included distorted/recrystallized grains/grain boundaries, sub-boundaries, and twins.

Selected portions of low-resolution, normal-direction IPF maps illustrating the grain structures after 50%, 75% and 93% reduction are shown in Fig. 2; for simplicity, only HABs are shown (as solid black lines). At the two lower reductions (Fig. 2a, b), it is evident that extensive grain compression occurred during cryogenic rolling, thus transforming the original low-aspect-ratio grains into a highly-elongated pancake-shape grain structure. To quantify this effect, the mean HAB intercept in the ND was estimated as a function of the rolling deformation by using the RD-ND samples (Fig. 3). For comparison purposes, the theoretically-predicted geometric reduction of the grain thickness due to the imposed rolling strain is also shown as a broken line. The measured grain thickness closely follows the theoretically-predicted curve initially (Fig.

[2] The reader is referred to on-line version of the paper to see the figures in color.

3), thus indicating that the observed reduction in the HAB spacing is largely a geometrical effect caused by compression and extension of pre-existing boundaries in proportion to the shape change of the sample. However, at reductions higher than 50%, the grain intercept length deviates significantly from the prediction based on homogeneous deformation (Fig. 3). This transition is mirrored in the microstructures represented by the IPF maps (Figs. 2b, c). Fine, equiaxed grains appeared to be generated along the original grain boundaries, thereby producing a “necklace”-type structure reminiscent of discontinuous dynamic/static recrystallization at elevated temperatures in metallic materials. Thus, it may be concluded that a second physical mechanism in addition to the geometrical effect is entailed in grain-structure evolution in cryogenically-rolled copper.

Higher-resolution EBSD maps (e.g., Fig. 4) provided deeper insight into the process of grain structure development; in these maps, LABs are depicted as thin red lines, and HABs as solid black lines. The EBSD maps showed that that a number of the original grain boundaries exhibited local bulges, some of which appeared to have transformed into fine equiaxed grains (some of which are indicated by arrows). This effect was apparent even after relatively small deformation (Fig. 4a). It became more pronounced with strain when the fraction of fine equiaxed grains increased noticeably, and the “necklace” microstructure developed (Fig. 2b, c, 4c). These fine grains are completely surrounded by HABs and typically contain almost no substructure (Fig. 4c). Therefore, the formation of fine grains appears to fit the definition of the discontinuous recrystallization controlled by nucleation and growth due the migration of boundaries. Because the samples warmed following rolling and were examined under similar ambient conditions, however, it is difficult to determine whether such recrystallization was dynamic/metadynamic at the rolling temperature or metadynamic/static at room temperature. This aspect is discussed further in Section 3.5.

TEM observations of the heavily-rolled material (Fig. 5) also suggested the occurrence of discontinuous recrystallization. In some regions, the microstructure was dominated by high dislocation density and sharp contrast variations indicative of significant elastic strains (Fig. 5a), or features often found in severely-deformed materials. In other areas (Fig. 5b), dislocation-free, *recrystallized* grains exhibiting reasonably homogeneous TEM contrast and containing annealing twins (arrows) were found.

Fig. 4 also reveals that sub-boundaries were also developed in cryogenically-rolled material. In some cases, the sub-boundaries extended across the parent grains, forming more or less regular arrays of nearly parallel bands aligned in a common direction. Examples of such structures are given in the high-magnification inserts in Figs. 4a, b, c. The EBSD results showed that some segments of such sub-boundaries accumulated misorientations in excess of 15°. These observations may be interpreted in terms of a grain-subdivision process [15] or/and micro-shear banding. The boundary planes of the sub-boundaries were usually far from {111} slip plane traces (shown by the dotted lines in the high-magnification inserts); this observation differs from some literature data [11]. Most of the sub-boundaries, however, were short and curved, tended to cluster near original grain boundaries, and had relatively small misorientations (Fig. 4). The contours of the original grains were clearly seen even after large rolling reductions (Figs. 2 and 4), thus suggesting that grain subdivision/shear banding was not a significant contributor to grain refinement.

Another important microstructural feature noted in the cryogenically-rolled material was twinning. Several examples of twins are circled in Fig. 4; more detailed statistics for the twin boundaries (derived from much larger EBSD scans) are summarized in Table 1. After 50 and 75% reduction, the shape of the twins appeared distorted, but their initial lens shape was still recognizable (Figs. 4a-b). Thus, it may be concluded that the twins originated during deformation in agreement with recent papers [7, 8] reporting the activation of the mechanical twinning during cryogenic deformation of copper. However, the present results indicate that the twin boundary fraction was relatively low (Table 1), and the twins were observed only sporadically (Fig. 4a, b). Hence, the contribution of twinning to the overall deformation was relatively low. The results in Table 1 also suggest that the twin boundary fraction *decreased* in the deformation range of 50 to 75% reduction. This effect can be ascribed to strain-induced deviation from the exact twin/matrix relationship and thus a gradual transformation of the twin boundaries into random HABs during deformation. This phenomenon has also been already reported in the literature [e.g., Reference 16] and may be explained as being due to the deformation-induced crystallographic rotations of the twins and matrix from their initial orientations. After yet higher rolling reduction (i.e., 93%), on the other hand, the twin fraction increased significantly (Table 1). The twins observed in the 93% rolled material had a rectangular shape (e.g., circled regions in Fig. 4c) which contrasted with the lenticular-shaped twins after 50 and 75% reduction (Fig. 4a, b). This rectangular morphology is often associated with *annealing* twins and may thus be inter-related with the above-mentioned discontinuous recrystallization that occurred after cryogenic rolling to high reductions.

The overall statistics from the grain-size measurements along the three principal directions of the rolled sheet are summarized in Table 2. In addition to the mean HAB intercept length, the average boundary spacing (including all boundaries with misorientations of at least 2°) is also shown. These results reveal that cryogenic rolling of copper provides significant refinement but the desirable NC grain sizes are not achieved. The present findings differ from recent literature [e.g., reference 8]. The difference in behavior may be due to the limited contribution of twinning and shear banding to microstructure evolution in present work. Further research is needed, however, to confirm whether this is an inherent feature of the cryogenic rolling of copper or a result of the fine-grained nature of the initial, rolling-preform material.

3.3. Misorientation distribution

To establish a better understanding of the grain-refinement process, misorientation data were derived from high-resolution EBSD maps (Fig. 6, Table 3). The misorientation-angle data shown in Fig. 6a are expressed in terms of the specific grain-boundary length, which equals the total grain-boundary *length* for a given misorientation angle (or small range of misorientation angles) divided by the area of the EBSD map. This metric provides a direct comparison of grain-boundary characteristics for the different rolling reductions, thus enabling more reliable deduction of the key physical mechanisms governing microstructure evolution. It should also be noted that the misorientation-angle data in Fig. 6a were obtained from the rolling plane. Due to compression of the parent grains (because of the geometrical requirements of strain), the specific grain-boundary length in the RD-TD plane should naturally decrease and

thus any evidence of the grain refinement (i.e., an increase in the HAB length) is readily detected.

After 50-75% reduction, the specific length of LABs increased significantly (Fig. 6a). This effect is associated with the extensive development of deformation-induced boundaries (DIBs) during cryogenic rolling, leading to a decrease in the total HAB fraction (Table 3) as well as to a reduction of the mean LAB misorientation (Fig. 6b). On the other hand, the specific length of HABs changed only slightly (Fig. 6a), indicating insufficient grain refinement at this strain level. The higher resolution inset in Fig. 6a reveals that the specific length of ~15-20^{o} boundaries rose compared to that in the initial material. This finding suggests that some DIBs achieved misorientations greater than 15°, thus transforming into HABs; examples of such boundaries are seen in the inserts in Figs. 4a, b. After 50% reduction, the specific length of ~25-55° boundaries decreased. This effect is most likely associated with the geometrical flattering of grains described in Section 3.2.

After 75% reduction, the specific length of ~25-55° boundaries showed an increase back to approximately the initial level. This process did not develop via the progressive movement of the low-angle peak toward higher misorientations. Rather, the specific length of HABs appears to have increased essentially uniformly over the entire misorientation range of ~25-55°. Therefore, it is likely that this effect can be associated with the bulging of original grain boundaries (several examples of which are indicated by the arrows in Fig. 4b), thereby giving rise to a homogeneous increase of the HAB area.

A shallow peak in the vicinity of 60° for material rolled to a reduction of 50-75% (Fig. 6a) is associated with the twin boundaries. Thus, the limited changes in this region confirm the above conclusion regarding the minor contribution of twinning to microstructure evolution.

After cryogenic rolling to a 93% reduction, the low-angle portion of the misorientation distribution did start to skew toward higher misorientations (Fig. 6a) and the mean LAB misorientation angle increased substantially (Fig. 6b). This observation indicates the progressive accumulation of misorientation across the DIBs. In addition, the specific length of the HABs increased significantly (Fig. 6a), thus providing evidence of grain refinement. In the misorientation range of ~15-55°, this process appears to have occurred reasonably homogeneously (Fig. 6a), thereby supporting the hypothesis of discontinuous grain nucleation and boundary migration rather than a continuous LAB-to-HAB transformation associated with so-called *continuous* dynamic recrystallization. The substantial sharpening of the 60° peak after 93% reduction (Fig. 6a) together with a doubling of the twin-boundary fraction (Table 1) are most likely attributable to the re-appearance of annealing twins.

3.4. Texture evolution

Rolling textures in FCC metals are often described in terms of two partial <110> fibers (the α-fibre with <110> parallel to the ND and the β-fibre with <110> tilted 60^{o} toward to the RD) and specific texture components (Fig. 7, Table 4). The fiber textures typically develop after small reductions. At higher reductions, the fibers tend to degenerate giving rise to pronounced, discrete peaks which may include the cube {100}<100>, Goss {011}<100>, brass {011}<211>, S {123}<412> or {123}<634>, or copper {112}<111> texture components (Table 4). The formation of the particular texture

components depends on the rolling temperature and material characteristics such as stacking-fault energy (SFE). During cold rolling, high SFE materials (including copper) usually exhibit the copper-type texture, whereas low SFE favors the formation of a brass-type texture.

In order to evaluate the texture developed during cryogenic rolling, orientation distribution functions (ODFs) were derived from the large EBSD scans containing ~15,000 grains each (Fig. 7). The development of individual texture components (within an angular spread of 15^{o} from the ideal orientation) as a function of strain is shown in Fig. 8.

After 50% reduction, the texture was weak (no peaks higher than ~3 x random), and the texture pattern could not be interpreted in terms of conventional rolling textures (Fig. 7); the small fractions of the main texture components were comparable to those in the initial material (Fig. 8). On the other hand, the remnants of the original cube texture were seen in the ODF (Fig. 7). In other words, the evolved texture seems to have been transient in nature after the 50% reduction.

In material rolled to the 75% reduction, the overall texture intensity was strengthened, and both fiber textures became evident in the ODF; the α-fiber appeared to be more pronounced than the β-fiber (Fig. 7). Within the α-fiber, Goss and brass texture components were noted, whereas the copper and S components were observed within the β-fiber (Fig. 7). The volume fractions of these components increased somewhat with reduction; the major components were the Goss and S textures (Fig. 8).

After 93% reduction, the texture became much sharper with the strongest peak being ~10 x random (Fig. 7). Furthermore, the fibers tended to separate into discrete components; i.e., the brass component of the α-fiber and the S component of the β-fiber (Fig. 7). This trend is quantified in Fig. 8; the fractions of the brass and S-textures increased at 93% reduction, Goss tended to saturate, and the copper component decreased markedly. Thus, the final texture was characterized by the predominance of the brass texture and noticeable proportions of the S and Goss components. Nevertheless, it should be emphasized that there was still substantial smearing about the specific ideal orientations (Fig. 7).

The present texture results contrast with those typically observed in copper after *ambient-temperature* rolling for which fiber textures develop after 50% reduction, and the main texture components are very sharp after 75-95% reduction [e.g. 19]. The texture evolved comparatively slowly during cryogenic rolling. Furthermore, the preferential development of the brass texture during cryogenic rolling contrasts with the copper texture typically developed at room temperature. A related temperature dependence has been reported recently for cryogenically-deformed aluminum [4]. In this regard, it is commonly thought that such effects are due to either extensive twinning and/or the suppression of cross slip [e.g. 20]. As discussed in Section 3.2, deformation twinning has been found to be minimal during cryogenic rolling of copper. On the other hand, cross slip, being a thermal-assisted process, may be inhibited at cryogenic temperatures and thus be the source of the observed formation of the brass texture. Moreover, low amounts of cross slip may also explain the limited amount of grain subdivision which is dependent on recovery-type processes.

Another important finding concerns the significant volume fraction of the S component in the final texture (Fig. 8). This component is frequently observed in rolled

FCC metals and is often explained in terms of the initial cube orientation of a material. For example, Hirsch and Lucke [17] have shown that the cube orientation rotates toward the S orientation during the development of the β-fiber texture. On the other hand, the rate of rotation of the cube orientation *toward* the β-fiber has been found to be much higher than the rate of movement *along* this fiber. Thus, a strong S orientation might be expected at an intermediate level of reduction [17]. Nevertheless, the development of stable end orientations during rolling is predicted to occur only at very high true strains ($\varepsilon \sim 5$), and therefore most of the experimentally-observed textures (including those in the present work) represent intermediate stages of texture evolution [17].

The Goss texture component is usually associated with recrystallization occurring during hot rolling or static annealing. Therefore, it may be hypothesized that its formation in the present work is due to discontinuous recrystallization which was discussed in Section 3.2. To examine this hypothesis, EBSD texture-component maps were calculated for the material rolled to 75 and 93% reduction (Fig. 9). These maps revealed that the fine-equiaxed grains decorating elongated original grain boundaries had *random* crystallographic orientations and were not associated with the Goss texture component. Rather, the Goss texture component is exhibited by coarse elongated grains. It is likely therefore that the Goss component is not due to recrystallization but rather an element of the development of the α-fiber (Fig. 7).

The results in Fig. 9 also reveal that the main texture components were more or less randomly dispersed throughout the microstructure. Grain-boundary misorientations may significantly be influenced by such spatial texture patterns. To assess the effect of the texture on HAB development, so-called “uncorrelated” (or texture-derived) misorientation-angle distributions were calculated for the high-angle range and compared with the measured HAB misorientation distributions (Fig. 10); for comparative purposes, a random misorientation distribution is also plotted in Fig. 10. In contrast to the real misorientation distributions displaying the misorientation data between neighbouring pixels in the EBSD maps, the uncorrelated distributions were calculated assuming no spatial correlation between pixels; in other words, all possible misorientations between the sampled pixels (including noncontiguous ones) were calculated. Fig. 10 demonstrates that the real distributions match reasonably well with the uncorrelated ones with the exception of the twin-induced peak near 60^{o}. The good correlation between these distributions indicates that the development of the HAB misorientations was indeed closely linked with the evolution of texture.

Because all texture measurements were made at the mid-thickness of the cryogenically-rolled sheets, possible texture inhomogeneity in the thickness direction was not quantified in the present work.

3.5. Recrystallization

Further insight into recrystallization behavior and microstructure stability was obtained from mechanical-property measurements. The effect of rolling strain on the strength characteristics is shown in Fig. 11a. These data revealed that the room-temperature strength decreased after 75% reduction. This observation is in line with the microstructure-characterization results (Figs. 2, 4 and 5) which showed evidence of recrystallization in the heavily rolled material. It is worth noting that the mean grain/subgrain size was noticeably refined for rolling reductions in the range of 75-93%

(Table 2). Hence, the observed softening is most likely associated with the reduction of dislocation density in recrystallized grains (Fig. 5b).

The occurrence of recrystallization in cryogenically-deformed copper has been reported previously and attributed to the warming of the material to the room temperature after deformation [21-23]. It is believed that static recrystallization is induced by a high concentration of defects (primarily vacancies) in the deformed material which significantly enhances grain-boundary mobility and serves as the driving force for boundary migration [21].

Microhardness measurements after various room-temperature storage-time intervals following rolling lent further credence to the conclusion that recrystallization in present experiments was indeed static (Fig. 11b). The microhardness decreased significantly after six months and was then found to be relatively unchanged. This result agrees well with literature data [21-23], thus demonstrating that recrystallization in the present work likely occurred after cryogenic rolling. In addition, it was found that the microhardness of the initial material (after *warm* "abc" deformation) also decreased substantially with time at ambient temperature (Fig. 11b). This observation is also suggestive of ambient-temperature-microstructural instability in severely-deformed copper. The occurrence of recrystallization during static storage at the room temperature has also been observed in severely-deformed high-purity aluminum [24].

True stress-true strain curves measured at cryogenic temperature (and corrected for friction effects [25]) exhibited a nearly constant flow-hardening rate (Fig. 11c). This observation suggests that softening associated with dynamic recovery was minimal. Furthermore, the absence of a flow stress maximum followed by flow softening indicates that discontinuous dynamic recrystallization also did not occur during cryogenic rolling. Hence. these observations support the conclusion that the observed discontinuous recrystallization was static in nature.

It is also noteworthy that the EBSD measurements discussed in this paper were obtained ~1.5 years after cryogenic rolling and thus most likely reflect a stable microstructure. In fact, TEM observations performed only *two days* after rolling revealed the presence of recrystallized grains (i.e., Fig. 5b), thus indicating the relatively rapid development of static recrystallization.

4. Conclusions

The EBSD technique has been employed to establish the microstructural response of pure copper to cryogenic rolling and to evaluate the potential of this approach for the production of NC materials. The main conclusions from this work are as follows:

(1) Grain-structure development during/after cryogenic rolling is a complex process including the geometrical effects of strain, *static* recrystallization, and limited amounts of grain subdivision and twinning. At rolling reductions of ~50%, microstructure evolution is driven mainly by simple grain compression in proportion to the imposed strain. At higher strains, however, recrystallization begins to play a significant, albeit competitive, role in grain-structure formation. Grain subdivision and twinning do not contribute substantially to grain refinement.

(2) Recrystallization is discontinuous in nature, being mainly governed by nucleation and grain-boundary migration to produce fine equiaxed, strain-free grains.

Recrystallization probably takes place after cryogenic deformation during static storage of rolled material at room temperature.

(3) The development of a {110}<112> brass-type texture instead of a copper-type texture suggests that cross-slip is suppressed at cryogenic temperatures. This effect is likely responsible for the limited formation of well-defined subgrains during deformation.

(4) Cryogenic deformation significantly reduces the mean grain size but a desirable NC range is not achieved by such means. Grain-refinement is mainly associated with recrystallization and is probably a post-deformation effect. The low microstructural stability of cryogenically-rolled material suggests that such a processing approach may not be a suitable for the production of an NC structure in pure copper. On the other hand, the incorporation of second-phase particles in copper alloys may retard recrystallization following cryogenic deformation and give rise to an NC microstructure.

Acknowledgments

The authors would like to acknowledge Professor G.A. Salishchev for suggesting this research. They also are grateful to Dr. R.M. Galeyev and Dr. O.R. Valiakhmetov for providing the material used in this work and Dr. R.R. Daminov for technical assistance.

References

[1] R.Z. Valiev, I.V. Alexandrov, Nanostructured materials produced by severe plastic deformation, Moscow, Logos, 2000, 272 p.

[2] P.B. Prangnell, J.R. Bowen, P.J. Apps, Ultra-fine grain structures in aluminium alloys by severe deformation processing, Mater. Sci. Eng. A 375–377 (2004) 178–185.

[3] F. J. Humphreys, P. B. Prangnell, J. R. Bowen, A. Gholinia, C. Harris, Developing stable fine-grain microstructures by large strain deformation, Phil. Trans. R. Soc. Lond. A 357 (1999) 1663-1681.

[4] Y. Huang, P.B. Prangnell, The effect of cryogenic temperature and change in deformation mode on the limiting grain size in a severely deformed dilute aluminium alloy, Acta Mater. 56 (2008) 1619–1632.

[5] S.K. Panigrahi, R. Jayaganathan, A study on the mechanical properties of cryorolled Al-Mg-Si alloy, Mater. Sci. Eng. A. 480 (2008) 299-305.

[6] S.K. Panigrahi, R. Jayaganathan, V. Chawla, Effect of cryorolling on microstructure of Al-Mg-Si alloy, Mater. Letter. 62 (2008) 2626-2629.

[7] Y.S. Li, N.R. Tao, K. Lu, Microstructural evolution and nanostructure formation in copper during dynamic plastic deformation at cryogenic temperatures, Acta Mater. 56 (2008) 230–241.

[8] Y. Zhang, N.R. Tao, K. Lu, Mechanical properties and rolling behaviors of nano-grained copper with embedded nano-twin bundles, Acta Mater. 56 (2008) 2429–2440.

[9] A.M. Hodge, Y.M. Wangb, T.W. Barbee, Mechanical deformation of high-purity sputter-deposited nano-twinned copper, Scripta Mater. 59 (2008) 163–166.

[10] Y. Estrin, N.V. Isaev, S.V. Lubenets, S.V. Malykhin, A.T. Pugachov, V.V. Pustovalov, E.N. Reshetnyak, V.S. Fomenko, L.S. Fomenko, S.E. Shumilin, M. Janecek, R.J. Hellmig, Effect of microstructure on plastic deformation of Cu at low homologous temperatures, Acta Mater. 54 (2006) 5581–5590.

[11] Z. Jasiefiski, H. Paul, A. Pittkowski, A. Litwora, Microstructure and Texture of Copper Single Crystal of (112)[111] Orientation Undergoing Channel-Die Compression at 77 K, J. Mater. Proc. Techn. 53 (1995) 187-194.

[12] J. A. Hines and K. S. Vecchio, Recrystallization kinetics within adiabatic shear bands, Acta Mater. Vol. 45, No. 2, pp. 635-649, 1997.

[13] S,V, Dobatkin, G.A. Salischev, A.A. Kuznetsov, T.N. Kon'kova, Submicrocrystalline structure in copper after different severe plastic deformation schemes, Mater. Sci. Forum 558-559 (2007) 189-194.

[14] TSL. OIM Version 3.0. On-line help. Draper, UP: TSL; 2001.

[15] D. A. Hughes and N. Hansen, High angle boundaries formed by grain subdivision mechanisms, Acta Mater. 45 (1997) 3871-3886.

[16] Ye.V. Nesterova, V.V. Rybin, Mechanical twinning and the fragmentation of commercial titanium at the stage of developed plastic deformation, Phys. Met. Metall. 59 (1985) 169-179.
[17] J. Hirsch and K. Lucke, Mechanism of deformation and development of rolling textures in polycrystalline F.C.C. metals – II. Simulation and interpretation of experiments on the basis of Tylor-type theories, Acta Metall. 36 (1988) 2883-2904.
[18] Y. Zhou, K.W. Neale, L.S. Toth, Analytical solutions for the ideal orientations of F.C.C. rolling textures, Acta Metall. Mater. 39 (1991) 2921-2930.
[19] J. Hirsch, K. Lucke, Mechanism of deformation and development of rolling textures in polycrystalline F.C.C. metals – I. Description of rolling texture development in homogeneous CuZn alloys, Acta Metall. 36 (1988) 2863-2882.
[20] I.L. Dillamore, W.T. Roberts, Rolling textures in F.C.C. and B.C.C. metals, Acta Metall. 12 (1964) 281-293.
[21] H.D. Meingelberg, M. Meixner, K. Lucke, The kinetics of the recrystallization of copper deformed at low temperatures, Acta Metal. 13 (1965) 835-844.
[22] I.A. Gindin, V.K. Aksenov, I.F. Borisova, Ya.D. Starodubov, Features of the low temperature recrystallization of copper, Phys. Met. Metall. 39 (1975) 72-77.
[23] I.A. Gindin, Ya.D. Starodubov M.P. Starolat, P.A. Khaymovich, Features of the defect structure of low-temperature extruded copper, Phys. Met. Metall. 48 (1979) 89-94.
[24] A.A. Salem, T.G. Langdon, T.R. McNelley, S.R. Kalidindi, and S.L. Semiatin, Strain-path effects on the evolution of microstructure and texture during the severe-plastic deformation of aluminum, Metall. Mater. Trans. A 37 (2006) 2879-2891.
[25] S.L. Semiatin, M.W. Corbett, P.N. Fagin, G.A. Salishchev, and C.S. Lee, Dynamic-coarsening behavior of an α/β titanium alloy, Metall. Mater. Trans. A 37 (2006) 1125-1136.

Table 1. Effect of cryogenic rolling on twin-boundary area fraction

Material Condition	Fraction (5-deg tolerance), %	
	Rolling plane	Longitudinal plane
Initial		4.8
50% reduction	4.7	3.5
75% reduction	2.9	2.8
93% reduction	5.6	6.0

Table 2. Effect of cryogenic rolling on mean grain-boundary intercept length

Material Condition	Mean HAB intercept length, μm			Mean grain-boundary intercept length (including LABs and HABs), μm		
	RD	ND	TD	RD	ND	TD
Initial	1.8	1.6	-	1.2	1.1	-
50% reduction	2.3	0.8	1.8	0.6	0.4	0.6
75% reduction	2.0	0.6	1.7	0.5	0.3	0.4
93% reduction	0.9	0.5	0.6	0.5	0.3	0.3

Table 3. Effect of cryogenic rolling on HAB area fraction

Material Condition	HAB fraction, %	
	Rolling plane	Longitudinal plane
Initial		59
50% reduction	21	27
75% reduction	20	33
93% reduction	42	50

Table 4. Euler angles and Miller indices of the ideal orientations in rolling textures of FCC metals (after Zhou, et al. [18])

Orientation	Euler angles, deg (Bunge convention)			Rolling plane	Rolling direction
	φ_1	Φ	φ_2		
Cube	0	0	0	(001)	$[0\bar{1}0]$
Goss	0	45	90	(101)	$[0\bar{1}0]$
Brass	35.3	45	90	(101)	$[\bar{1}\bar{2}1]$
S_1	56.8	29.2	63.4	(214)	$[\bar{1}\bar{2}1]$
S_3	59.0	36.7	63.4	(213)	$[\bar{3}\bar{6}4]$
Copper	90	35.3	45	(112)	$[\bar{1}\bar{1}1]$
Taylor	90	27.4	45	$(4;4;11)$	$[\bar{1}\bar{1};\bar{1}\bar{1};8]$

Figure Captions

Figure 1. Characterization of the copper program material prior to cryogenic rolling: (a) EBSD inverse-pole-figure map, (b) misorientation distribution (misorientation-axis distribution is shown in the top right corner), and (c) (100), (110) and (111) pole figures illustrating texture.

Figure 2. Selected portions of low-resolution, inverse-pole-figure maps measured following cryogenic rolling to a reduction of (a) 50% (longitudinal plane), (b) 75% (longitudinal plane), or (c) 93% (rolling plane). For simplicity, only HABs are shown in the maps.

Figure 3. Dependence of the mean HAB intercept in the ND on rolling reduction. The broken line shows a theoretically-predicted curve calculated from the geometrically required shape change associated with the imposed strain.

Figure 4. Selected portions of high-resolution EBSD maps taken on the rolling plane of samples cryogenically rolled to reductions of (a) 50%, (b) 75%, or (c) 93%. The high-magnification insert in each figure delineates the degree of grain subdivision.

Figure 5. TEM images of microstructure developed in copper cryogenically rolled to a reduction of 75%: (a) Heavily deformed microstructure and (b) recrystallized microstructure.

Figure 6. Effect of rolling reduction on (a) the misorientation-angle distribution and (b) the mean LAB misorientation angle. In (a), the insert shows the high-angle region of the distribution in more detail.

Figure 7. Schematic representation of FCC rolling textures in Euler-angle space (after Hirsch and Lucke [17]) and experimental ODFs after a reduction of 50, 75, or 93% via cryogenic rolling.

Figure 8. The evolution of rolling-texture components (within 15° of the ideal orientations) as a function of the rolling reduction.

Figure 9. Spatial distributions of the main texture components (within 15° of the ideal orientations) in copper cryogenically rolled to a reduction of (a) 75% (longitudinal plane) or (b) 93% (rolling plane).

Fig. 10. Comparison of the high-angle portions of the grain-boundary misorientation distributions and (uncorrelated) texture-derived distributions for material cryogenically rolled to a reduction of (a) 75% or (b) 93%.

Figure 11. Effect of cryogenic-rolling reduction and period of time following deformation on yield strength, ultimate tensile strength, and microhardness at room temperature (a and b, respectively) and (c) compression behavior of the material at cryogenic and ambient temperatures. In (a), the microhardness was measured 2 days after cryogenic rolling whereas the yield and ultimate tensile strength were measured 4 months after cryogenic rolling.

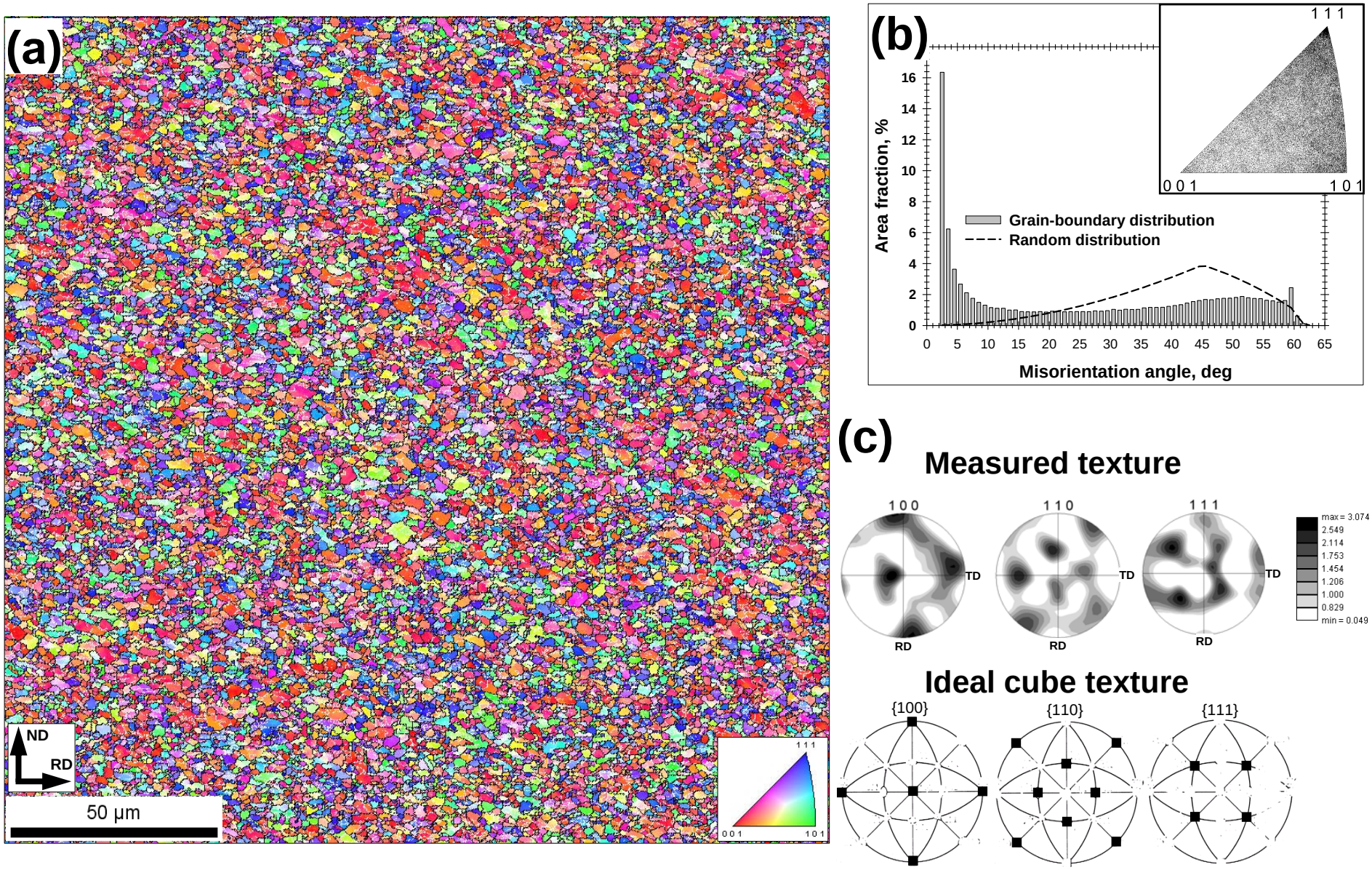

Figure 1. Characterization of the copper program material prior to cryogenic rolling: (a) EBSD inverse-pole-figure map, (b) misorientation distribution (misorientation-axis distribution is shown in the top right corner), and (c) (100), (110) and (111) pole figures illustrating texture.

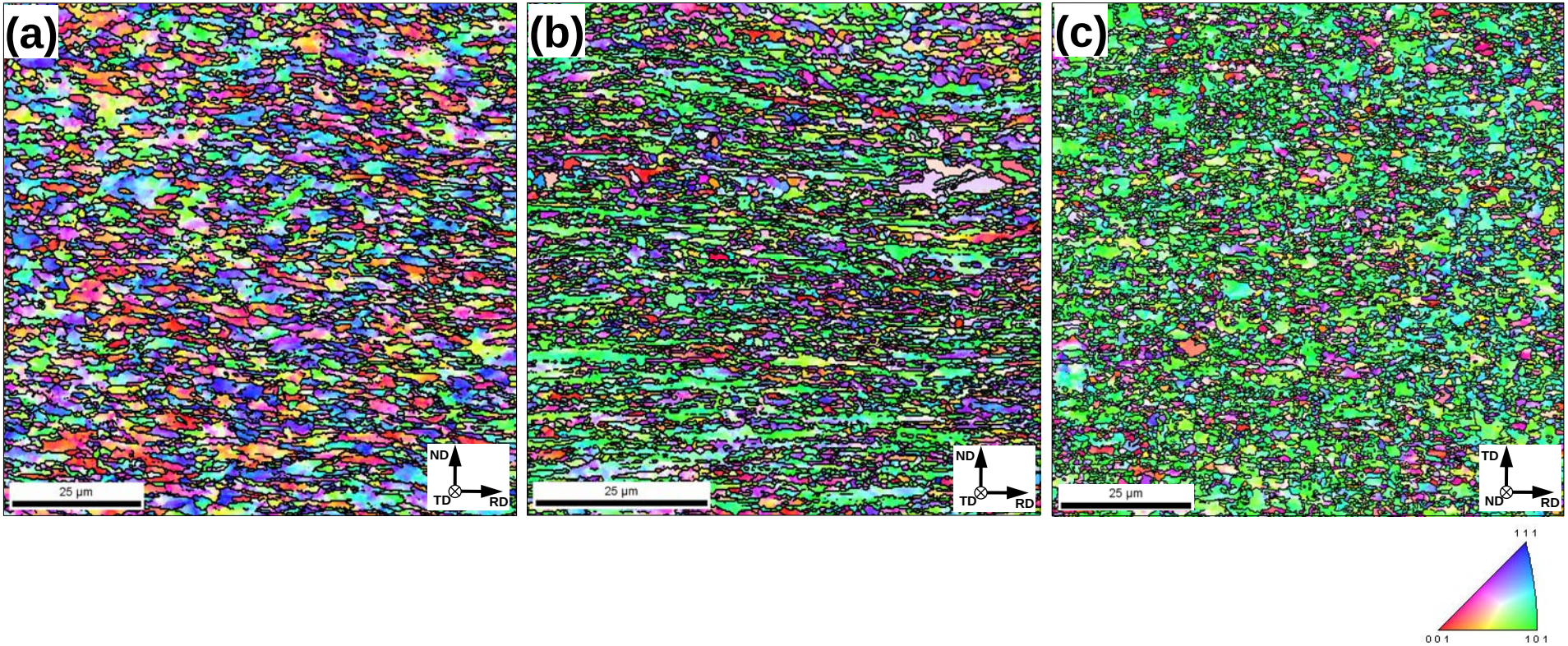

Figure 2. Selected portions of low-resolution, inverse-pole-figure maps measured following cryogenic rolling to a reduction of (a) 50% (longitudinal plane), (b) 75% (longitudinal plane), or (c) 93% (rolling plane). For simplicity, only HABs are shown in the maps.

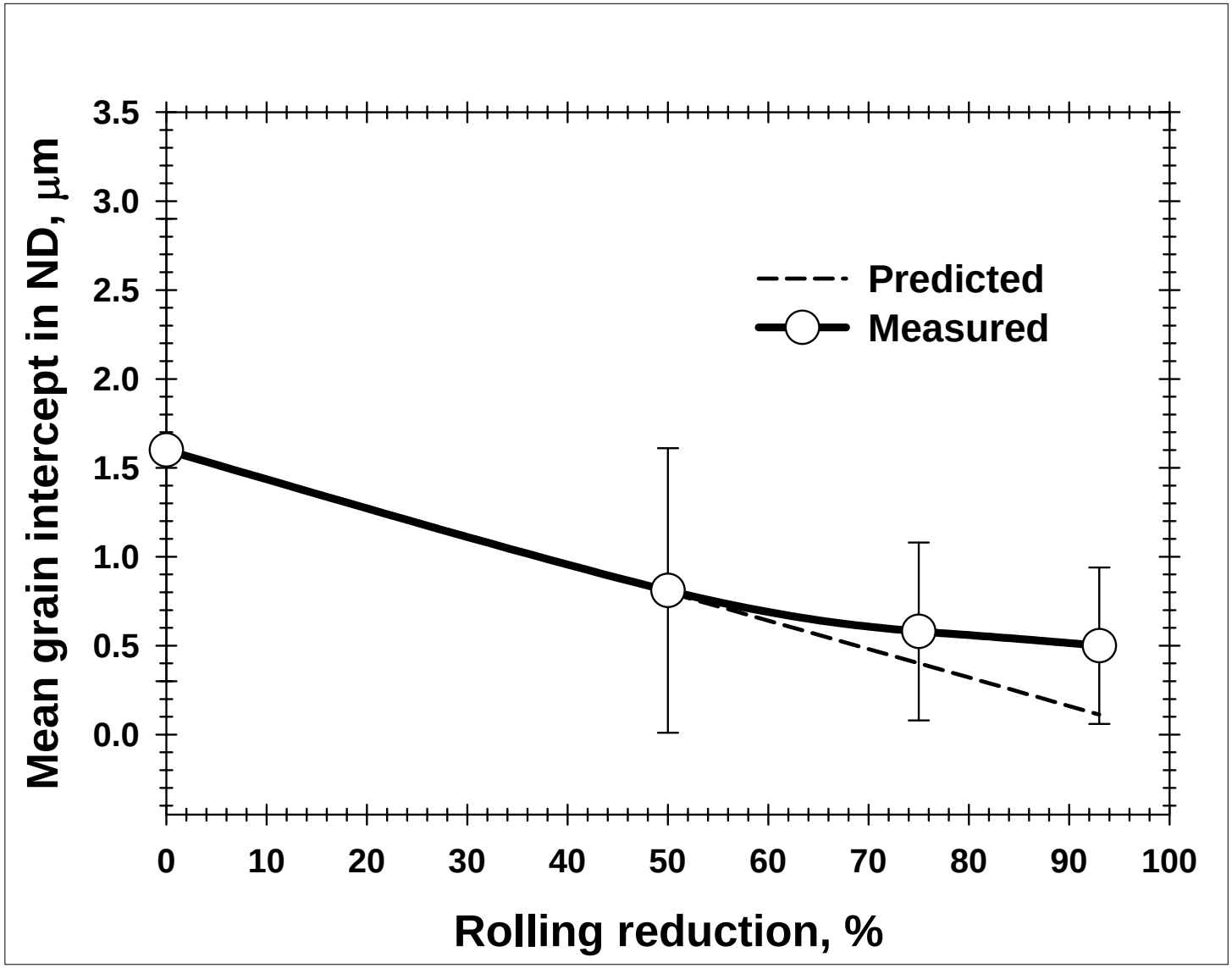

Figure 3. Dependence of the mean HAB intercept in the ND on rolling reduction. The broken line shows a theoretically-predicted curve calculated from the geometrically required shape change associated with the imposed strain.

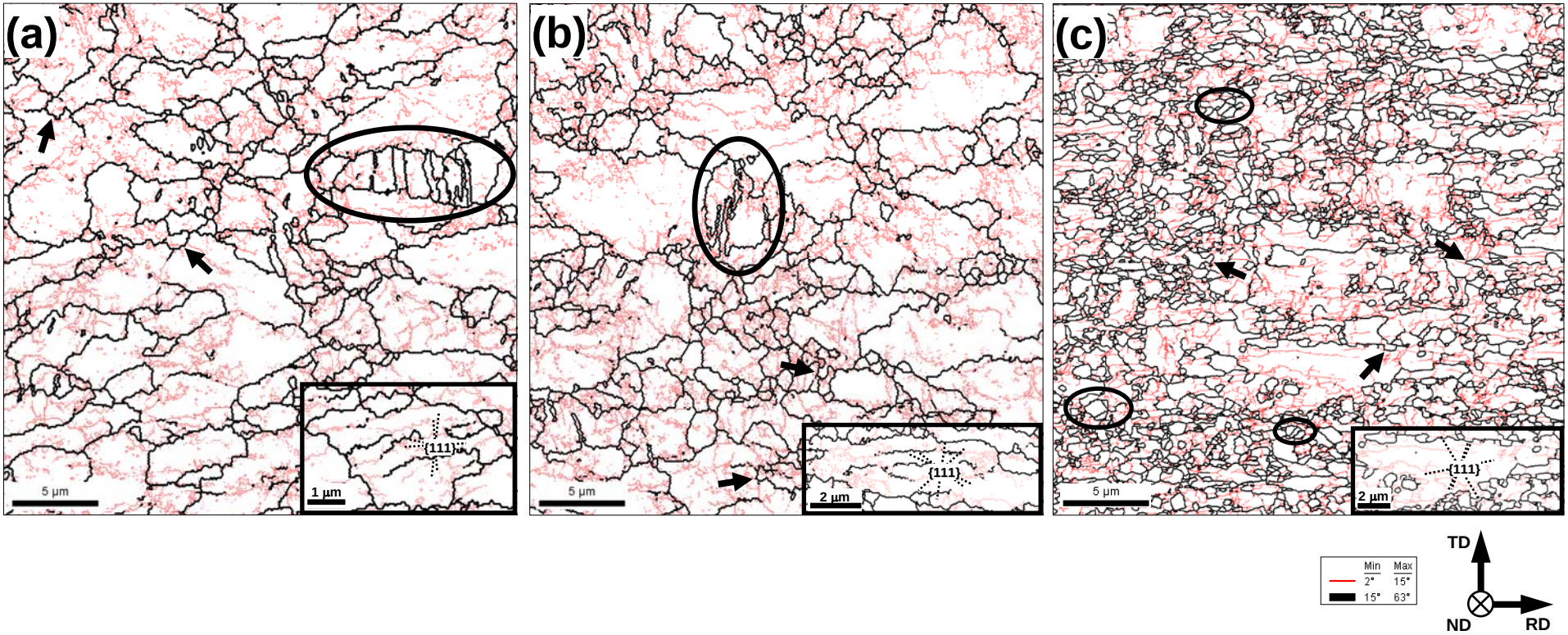

Figure 4. Selected portions of high-resolution EBSD maps taken on the rolling plane of samples cryogenically rolled to reductions of (a) 50%, (b) 75%, or (c) 93%. The high-magnification insert in each figure delineates the degree of grain subdivision.

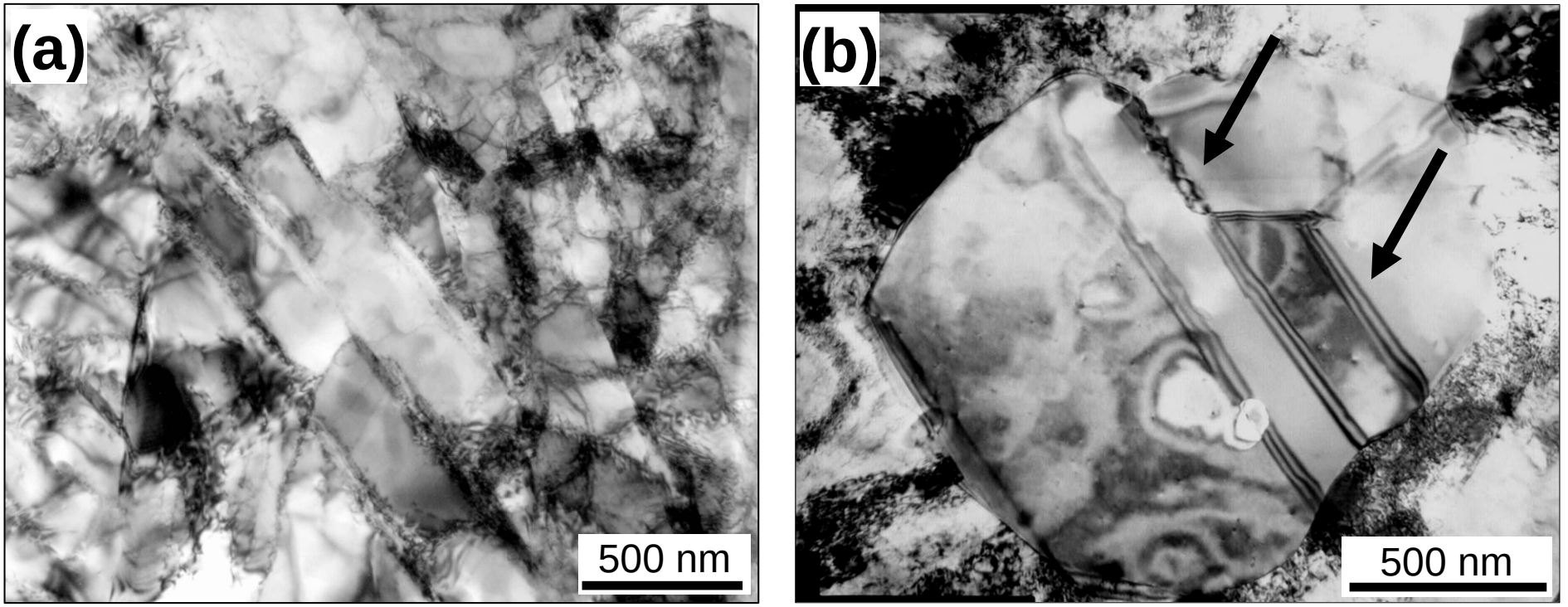

Figure 5. TEM images of microstructure developed in copper cryogenically rolled to a reduction of 75%: (a) heavily deformed microstructure and (b) recrystallized microstructure.

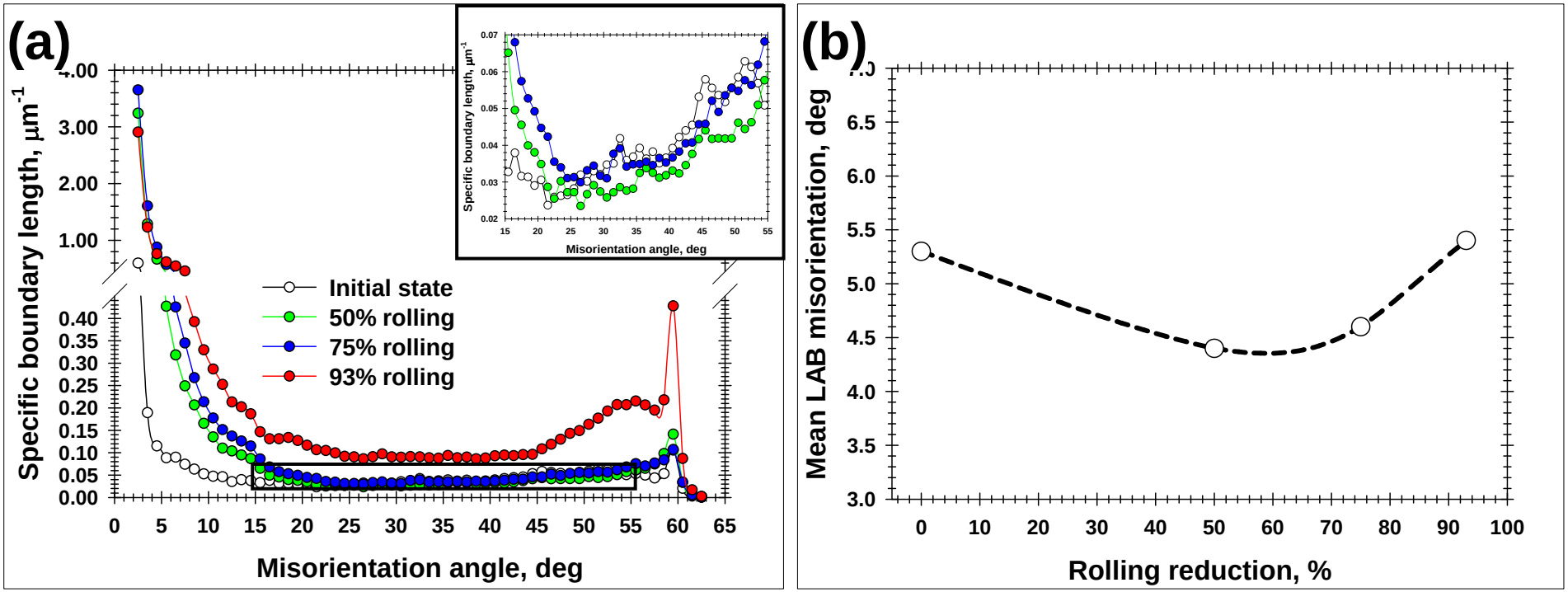

Figure 6. Effect of rolling reduction on (a) the misorientation-angle distribution and (b) the mean LAB misorientation angle. In (a), the insert shows the high-angle region of the distribution in more detail.

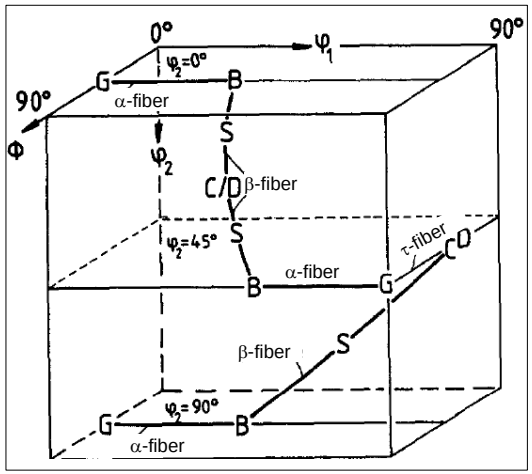

Ideal FCC rolling textures

G – Goss texture,
B – Brass texture
S – S-texture,
C – Copper texture
D-Taylor texture

50% rolling **75% rolling** **93% rolling**

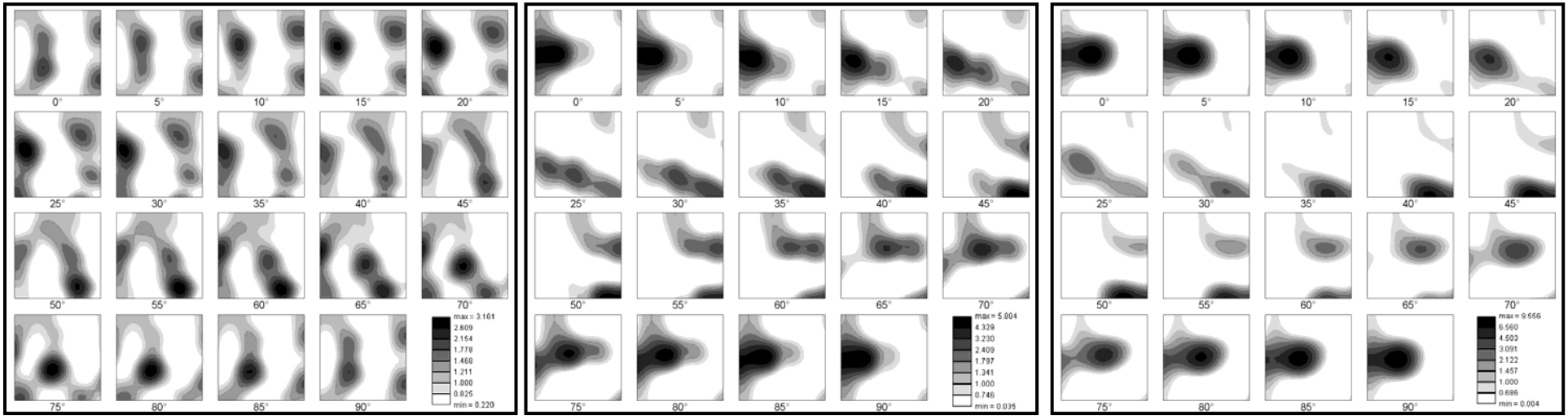

Figure 7. Schematic representation of FCC rolling textures in Euler-angle space (after Hirsch and Lucke [17]) and experimental ODFs after a reduction of 50, 75, or 93% via cryogenic rolling.

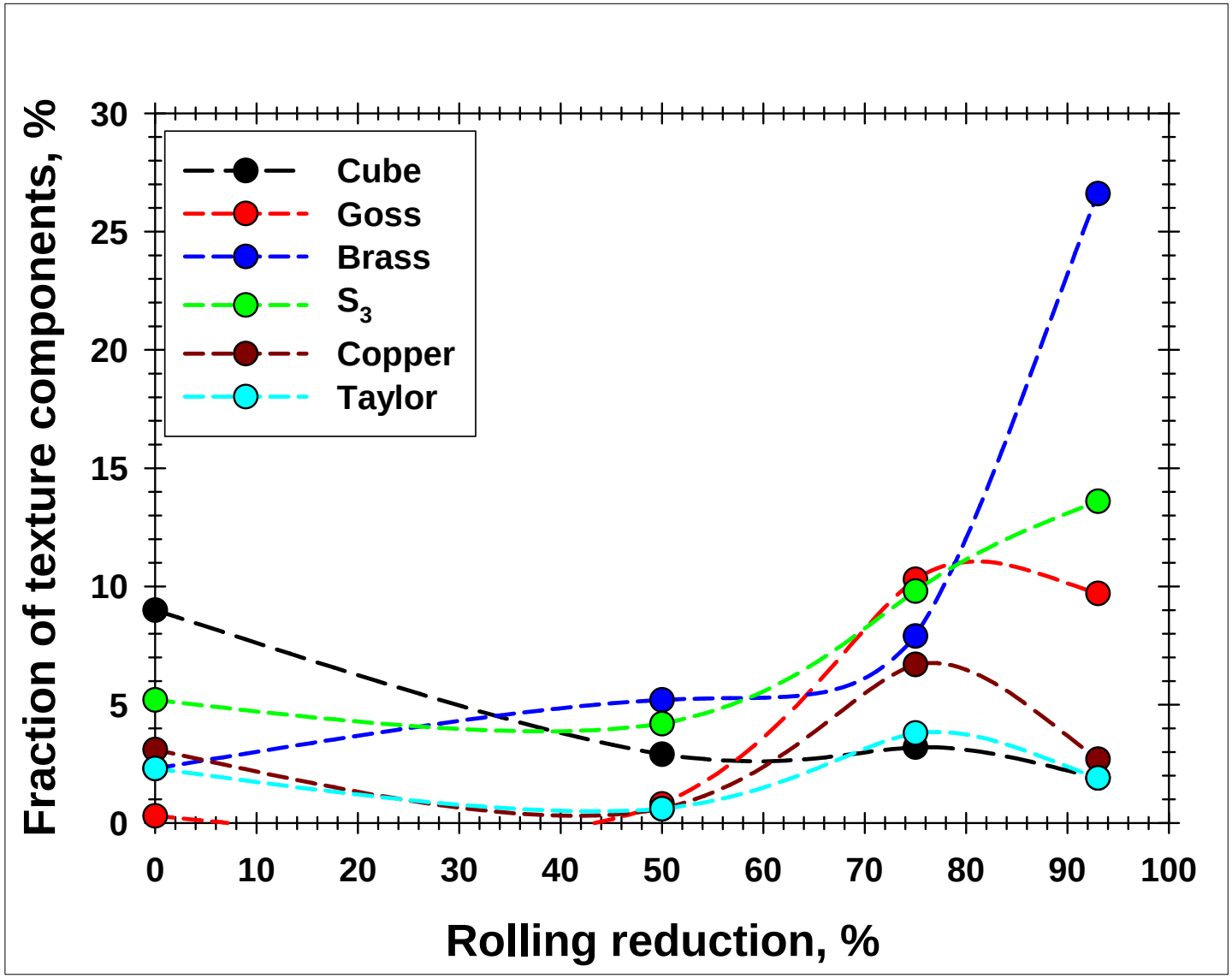

Figure 8. The evolution of rolling-texture components (within 15° of the ideal orientations) as a function of the rolling reduction.

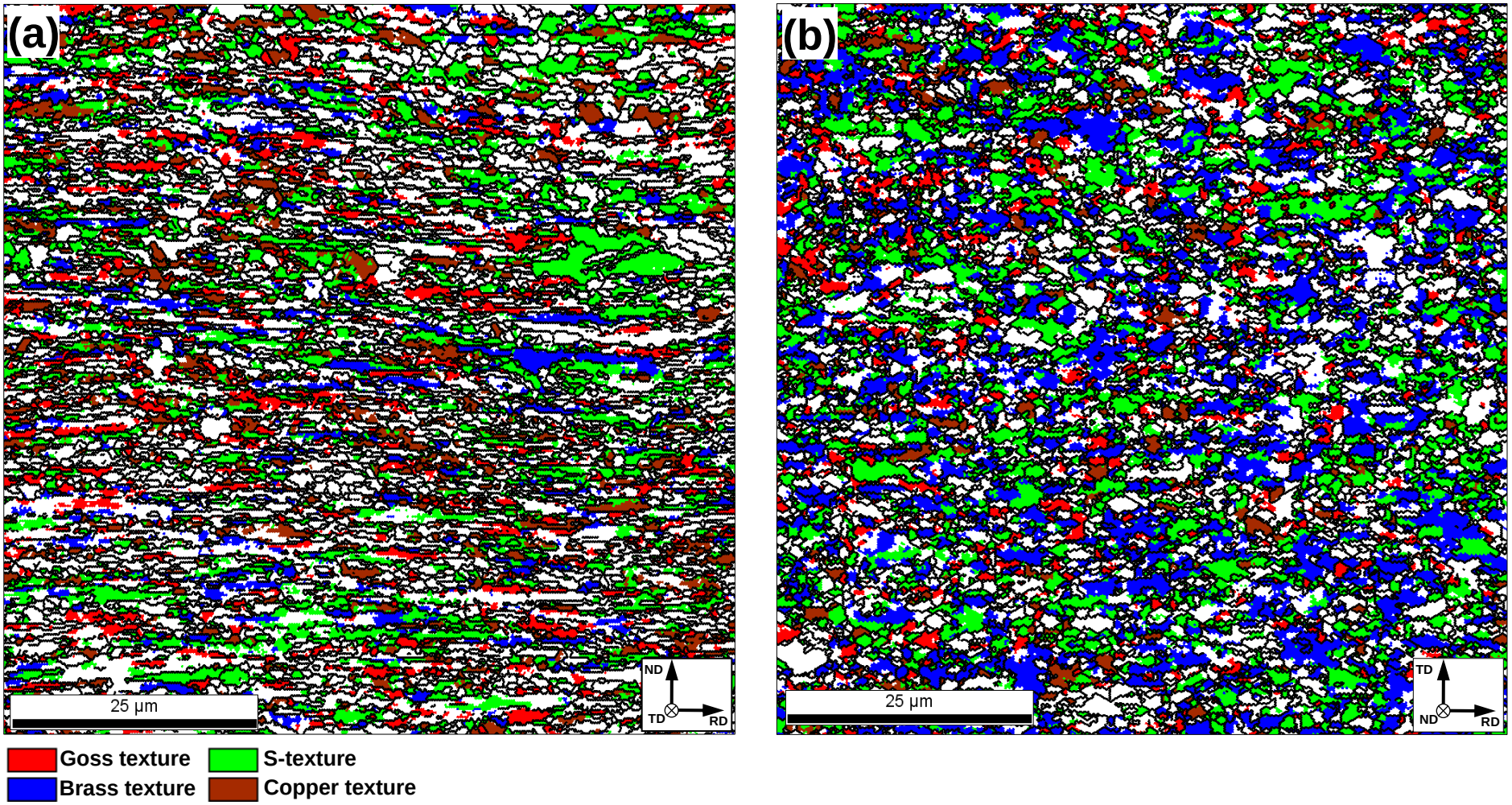

Figure 9. Spatial distributions of the main texture components (within 15° of the ideal orientations) in copper cryogenically rolled to a reduction of (a) 75% (longitudinal plane) or (b) 93% (rolling plane)

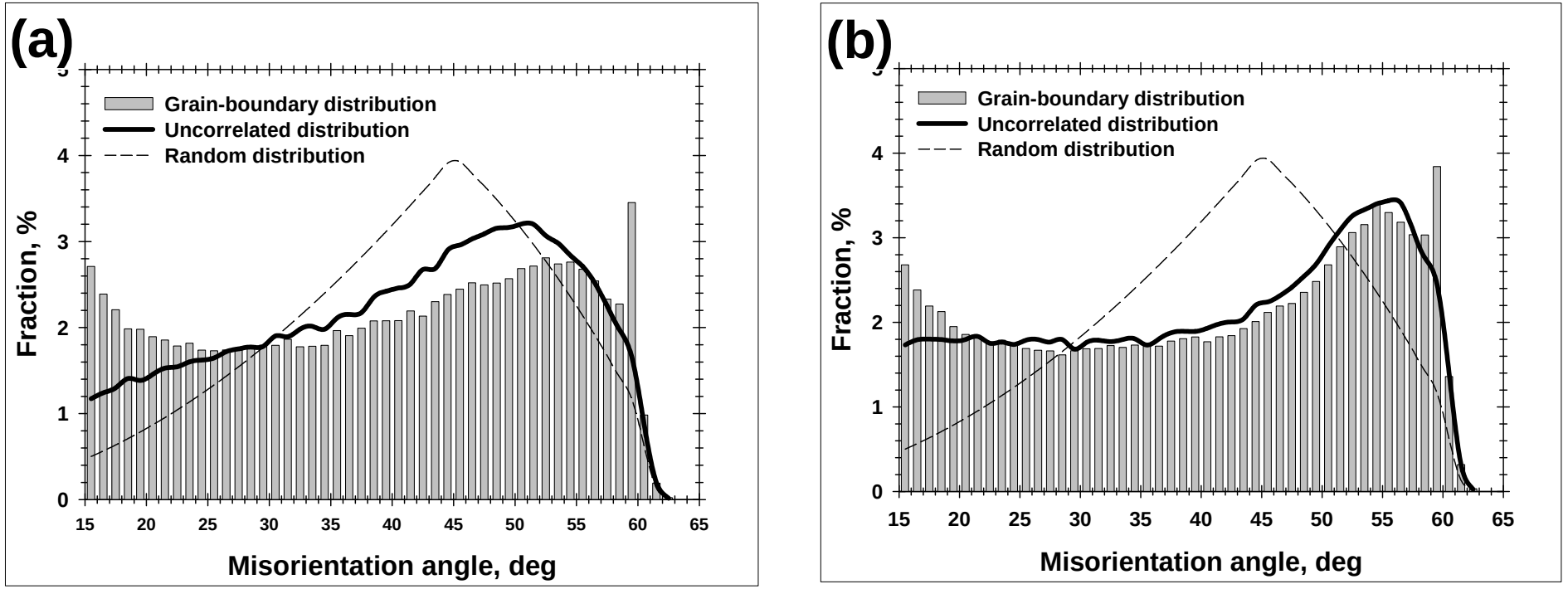

Fig. 10. Comparison of the high-angle portions of the grain-boundary misorientation distributions and (uncorrelated) texture-derived distributions for material cryogenically rolled to a reduction of (a) 75% or (b) 93%.

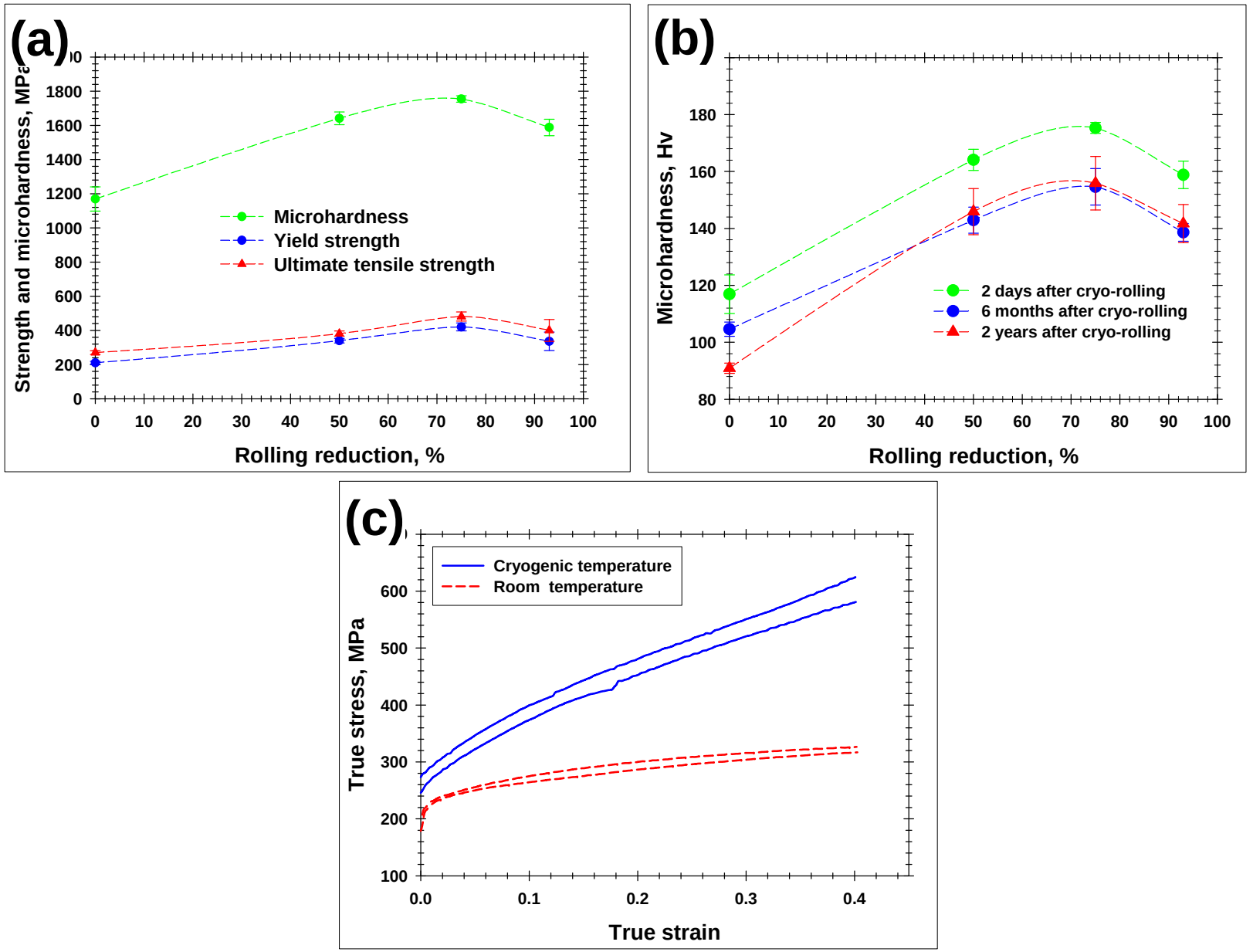

Figure 11. Effect of cryogenic-rolling reduction and period of time following deformation on yield strength, ultimate tensile strength, and microhardness at room temperature (a and b, respectively) and (c) compression behavior of the material at cryogenic and ambient temperatures. In (a), the microhardness was measured 2 days after cryogenic rolling whereas the yield and ultimate tensile strength were measured 4 months after cryogenic rolling.